RSC Advances

COMMUNICATION

View Article Online
View Journal | View Issue

Cite this: *RSC Adv.*, 2016, **6**, 114491

Received 2nd August 2016
Accepted 22nd November 2016

DOI: 10.1039/c6ra19514h

www.rsc.org/advances

Design, synthesis and biological evaluation of methyl-2-(2-(5-bromo benzoxazolone)acetamido)-3-(1*H*-indol-3-yl)propanoate: TSPO ligand for SPECT†

Pooja Srivastava,*[ab] Ankur Kaul,[a] Himanshu Ojha,[a] Pravir Kumar[b] and Anjani K. Tiwari*[a]

The translator protein (TSPO, 18 kDa), a transmembrane mitochondrial protein, has been explored as an important biomarker by researchers because of its involvement in inflammation, immune modulation and cell proliferation. Recently, our group has explored a modified benzoxazolone derivative for diagnostic applications that has overcome few problems of first and second generation TSPO PET ligands. In this study, a new skeleton acetamidobenzoxazolone–indole, a conjugation of two TSPO pharmacophoric moieties benzoxazolone and indole, has been designed, synthesized and evaluated for TSPO targeting for SPECT. The methyl-2-(2-(5-bromo benzoxazolone)acetamido)-3-(1*H*-indol-3-yl)propanoate (MBIP) ligand was designed on the basis of pharmacophore modeling done on benzoxazolone based TSPO ligands which was then validated computationally for TSPO binding through docking studies (PDB ID: 4RYO, 4RYQ, and 4UC1) which showed a comparable Glide G_{score} as compared to known ligands like PK11195, PBR28, and FGIN-127. MBIP was synthesized by amidation reaction of 2-(5-bromo-benzoxazolone)acetic acid with tryptophan methyl ester hydrochloride (yield 62%). The compound was synthesized and characterized using spectroscopic techniques like ^{1}H-NMR, ^{13}C-NMR, and mass spectroscopy. Purification was carried out by column chromatography and analytical HPLC (purity > 97%). The purified compound was labelled with ^{99m}Tc (radiochemical yield > 96%). The radiolabelled compound showed >94% stability in solution and >91% stability in serum after 24 h indicating the stable nature of the radio complex. A biodistribution study on BALB/c mice showed uptake of ^{99m}Tc-MBIP in TSPO rich organs and appropriate pharmacokinetics of excretion and release for a SPECT agent. Further evaluation of the ^{99m}Tc-MBIP may prove it as a potential candidate for TSPO targeting using SPECT.

1. Introduction

Inflammation is linked to the preliminary stage of many complications of diseases associated with lung inflammatory diseases, chronic obstructive pulmonary disease, acute liver damage, immune response to heart, brain injury, neurodegenerative diseases, psychiatric disorders and cancer.[1–8] Peripheral benzodiazepine receptor (PBR), renamed as translocator protein (TSPO, 18 kDa),[9] has been found to be an important biomarker for inflammation in the TSPO enriched organs. Recent investigations of TSPO in various biological processes and its importance in certain pathological situations due to altered concentration has led to development of various ligands for diagnostic purposes.[10–14]

Various radionuclides have been tried for diagnostic applications by targeting TSPO such as ^{11}C and ^{18}F for positron emission tomography (PET),[15–21] ^{123}I and ^{99m}Tc for single photon emission computed tomography (SPECT).[22–27] Other nuclides such as Eu^{3+} and Gd^{3+} have also been tried for optical and magnetic resonance imaging (MRI), respectively.[28,29] Different classes of TSPO ligands, for example, isoquinoline carboxamides, indoleacetamides, pyrazolopyrimidines, imidazolepyridines, benzodiazepines and benzoxazolone analogs have been developed.[30,31] Till date no ligand has been found ideal for human application throughout the globe. Few first generation ligands, such as PK11195 showed poor specificity and poor signal-to-noise ratio. Although second generation ligands, such as PBR28, DAA1106, DPA713, and PBR111 demonstrated improved signal-to-noise ratio but suffered from inter subject variability. This inter subject variability was attributed to rs6971 polymorphism in TSPO gene which results into single amino acid substitution *i.e.* Ala147Thr.[32] This amino acid substitution constitute three classes in terms of binding affinity: high affinity binder (HAB) having alanine at 147, low affinity binder (LAB) having threonine at 147 and mixed affinity binder (MAB) having alanine and threonine both. Low-binding affinity TSPO is present in 30% of Caucasians and 25% of Africans.[20]

[a]*Division of Cyclotron and Radiopharmaceutical Sciences, Institute of Nuclear Medicine and Allied Sciences, Brig. S. K. Mazumdar Road, Delhi-110054, India. E-mail: pshree_14@yahoo.co.in; anjani7797@rediffmail.com; Fax: +91-11-23919509; Tel: +91-11-23905362; +91-11-23905387*

[b]*Molecular Neuroscience and Functional Genomics Laboratory, Department of Biotechnology, Delhi Technological University, Delhi 110042, India*

† Electronic supplementary information (ESI) available. See DOI: 10.1039/c6ra19514h

^{11}C and ^{18}F labeling have their own limitations as they require on site cyclotron to produce the radioisotopes. ^{99m}Tc, an ideal single photon of 140 keV emitting radionuclide with half life of 6 h, has lesser radiation burden as compared to PET radionuclide and is generated through ^{99}Mo/^{99m}Tc generator. Although number of TSPO ligands have been synthesized but few of them have been modified for diagnostic purposes using metals for example ^{99m}Tc, ^{188}Re, Gd^{3+} and Eu^{3+} *etc.*[24–29] As these metal based ligands have been used for receptor targeting, this aspect can be further explored for TSPO. Some modification on quinoline carboxamide[25] and imidazolepyridines[24,26] have been reported with ^{99m}Tc for SPECT application which are the basis of TSPO ligands like analogues of PK11195 and CB86, respectively.

Recently, acetamidobenzoxazolone based skeleton, developed from first generation ligand RoS-4864 has been used by our group for the development of PET ligand [^{11}C]MBMP and [^{18}F]FEBMP with improved TSPO targeting properties over (R)[^{11}C]PK11195.[18–21] MBMP/FEBMP skeleton has shown favourable biodistribution pattern, high *in vitro* and *in vivo* specific binding for TSPO and has overcome the problem of intersubject variability. In our previous studies human postmortem brains of HABs and LABs were used for *in vitro* autoradiographic studies of MBMP/FEBMP. The binding ratios of (R)[^{11}C]PK11195, [^{11}C]DAA1106, [^{11}C]AC-5216, and [^{11}C]PBR28, for HAB to that of LAB were approximately 0.45, 1.19, 4.60, and 11.1, respectively, showing excellent correlation with the K_i ratios of these ligands for LAB to that of HAB. The compound [^{18}F]FEBMP has shown binding ratio of LAB to that of HAB as 0.9. This study presents [^{18}F]FEBMP as a promising TSPO ligand and skeleton for new ligands with negligible effect of rs6971 polymorphism on binding towards TSPO.[20]

Taking lead from this work, we have developed a new SPECT ligand using ^{99m}Tc for TSPO imaging. We have introduced a new skeleton acetamidobenzoxazolone indole propanoate as a TSPO ligand by conjugating acetamidobenzoxazolone moiety present in MBMP with indole moiety present in TSPO ligand, FGIN-127.[30] MBMP and FGIN-127 both display TSPO affinity in nanomolar range. The affinity of MBIP towards TSPO has been validated through docking studies using wild type as well as mutant PDBs of TSPO. Thereafter, newly designed potential TSPO ligand was synthesized through a simple and efficient four steps synthetic procedure which was characterized by NMR, mass and purified by HPLC. The purified compound was radiolabelled with ^{99m}Tc for biological evaluation. Stability of complex for *in vivo* application was evaluated in serum and biodistribution study was performed to evaluate its % uptake with time in TSPO enriched organs.

2. Materials and methods

2.1. Chemistry

2.1.1. Chemicals. All the chemicals and solvents were purchased from Sigma-Aldrich and Merck. ^{99m}Tc was procured from Regional Centre for Radiopharmaceuticals, Board of Radiation and Isotope Technology (BRIT), Department of Atomic Energy, India. Column chromatography was carried out using silica MN60 having mesh 60–120, thin layer chromatography (TLC) on aluminium plates coated with silica gel 60 F_{254} and instant thin layer chromatography silica gel (ITLC-SG) was used for identification of labeling, purity and R_f of radiocomplex.

2.1.2. Instrumentation. ^{1}H and ^{13}C NMR spectra were recorded on Bruker Avance II 400 MHz system at 400 MHz and 100 MHz, respectively. Mass spectroscopy was done on 6310 system of Agilent using ESI positive mode. γ-Scintigraphic studies were done on Hawkeye Camera and a γ-scintillation counter was used for counting radioactivity. High performance liquid chromatography (HPLC) was carried out on 1200 series of Agilent using analytical T3 Waters column (4.6 × 250 mm) for analysis and C-18 column (21.2 × 150 mm) for purification. SPECT images were taken on GE Triumph system.

2.1.3. Animal models. Animal protocols were approved by the Institutional Animal Ethics Committee (INM/DASQA/IAEC/09/015). BALB/c mice (22–28 g) were used for animal experiments.

2.1.4. Pharmacophore hypothesis generation. The pharmacophore hypothesis was developed by aligning pharmacophoric features of 51 TSPO ligands retrieved from the literature[33,34] using PHASE, Schrödinger, Maestro LLC 9.1 software. Generation of conformers was carried out with the help of MacromodelConfGen using OPLS2005 force field with rapid torsional search. Geometric alignment of site points in the active molecules to the site points in the hypothesis was the basis of hypothesis score generation. Each active molecule conformer generates hypothesis. Scores of the compounds were determined by 3D-QSAR model developed from compounds by aligning on the hypothesis. PLS analysis was carried out to evaluate the pharmacophore hypothesis using atom-based PHASE QSAR models generation with a maximum of three PLS factors for each pharmacophore type. Best hypothesis was further used for designing the TSPO ligand.

2.1.5. Docking studies. To design modified TSPO ligand, docking studies for ligand–protein interaction were carried out with extra precision (XP) mode of GLIDE, Schrödinger, Maestro LLC 9.1 software. Structures of ligands were drawn using ChemBioDraw. We have chosen wild type (4RYO and 4RYQ) as well as mutant (4UC1) PDBs for docking studies from different sources such as BcTSPO and RsTSPO. The rs6971 polymorphism in human resulting in A147T single amino acid change is equivalent to A139T in RsTSPO. Ultra 10.0.LigPrep and protein preparation modules were used for ligands and protein preparation, respectively. Protein preparation module consists of a series of steps that perform preprocess, optimization and minimization of protein structure. Receptor grids generation were required for docking with ligands. OPLS2005 forcefield has been used for the receptor grid as well as ligand grid generation. Docking simulation was performed in implicit solvent.

The ligand strain energy is the difference between the energy of the ligand as it is in the complex and the energy of the extracted ligand, minimized, starting from the geometry in the refined complex. This local strain energy is used for comparison of different poses of the same ligand. Calculations to assess the strain were performed in implicit solvent.

2.1.6. Synthesis

2.1.6.1 Synthesis of 2-(2-(5-bromo benzoxazolone)acetamido)-3-(1H-indol-3-yl)propanoate, 5 (MBIP). 2-(5-Bromo-benzoxazolone) acetic acid was synthesized as per Scheme 1 by following the procedure reported in the literature.[33] To a solution of 2-(5-bromo-benzoxazolone)acetic acid (250 mg, 0.92 mmol) in DMF (5 ml), tryptophan methyl ester hydrochloride (351.2 mg, 1.38 mmol), HOBt (124.2 mg, 0.92 mmol) and EDCl (264.3 mg, 1.38 mmol) were added at room temperature and stirred for 7 h. Subsequently, water was added and the mixture was extracted using a toluene and ethyl acetate (1 : 1). Water and brine were used for washing of organic layer and subsequently anhydrous Na_2SO_4 was added for drying. After filtration, the solvent was removed *in vacuo* and purification of residue was carried out on silica gel column chromatography using $CHCl_3$/EtOAc (4 : 1 v/v) as eluent to give amide as a white solid (MBIP: yield 62%). Chemical purity > 97% by HPLC: T3 column, 4.6 × 250 mm; MeCN/H_2O, 6/4–8/2 (v/v); flow rate: 0.8 ml min^{-1}; $\lambda_{uv} = 254$ nm; $t_R = 8.75$ min.

^{1}H-NMR (DMSO, 400 MHz): δ (ppm) 3.10–3.16 (2H, m), 3.59 (3H), 4.47–4.53 (3H, s), 7.00–7.50 (8H, m), 8.85–8.87 (1H, d), 10.90 (1H, s).

^{13}C-NMR (DMSO, 100 MHz): δ (ppm) 28.72 (CH_2–CH), 44.41 (CH_3–O), 52.44 (NH–CH–C=O), 53.91 (N–CH–C=O), 111–141.52 (14 carbon of aromatic rings), 154.15 (O–C=O–N), 166.28 (NH–C=O), 172.35 (O–C=O).

MS (ESI) *m/z*: 496.3 $[M + Na]^+$; calculated mass 496.38 $[M + Na]^+$.

2.1.6.2 Radiosynthesis. 200 μl solution of the compound (0.03 nM) was added in $SnCl_2 \cdot 2H_2O$ (1×10^{-2} M) (purged nitrogen 10% acetic acid (1 ml). Thereafter, 75 MBq, 100 μl saline solution of sodium pertechnetate (freshly eluted $NaTcO_4$) was added. The pH was adjusted to 7.0 by addition of 0.1 M $NaHCO_3$ solution to the reaction mixture and the contents were shaken manually. Vial was kept at room temperature for 20–30 min. ^{99m}Tc complex's labeling, chemical purity and R_f were determined by ITLC-SG strips by using developing solvents such as acetone and PAW (pyridine, acetic acid and water in 3 : 5 : 1.5 ratio) simultaneously. 0.1 cm segments of ITLC were taken for count measurement to find out the percentage of free and labeled ligand *i.e.* radiochemical purity.

2.1.7. *In vitro* serum stability assay. Blood was collected from healthy volunteers and was made to clot in a humidified incubator maintained at 5% carbon dioxide and 95% air at 37 °C for 1 h and was used to prepare serum. Centrifugation of sample at 400 rpm was followed by filtration through 0.22 μm syringe and filtrate was kept into sterile plastic culture tubes.

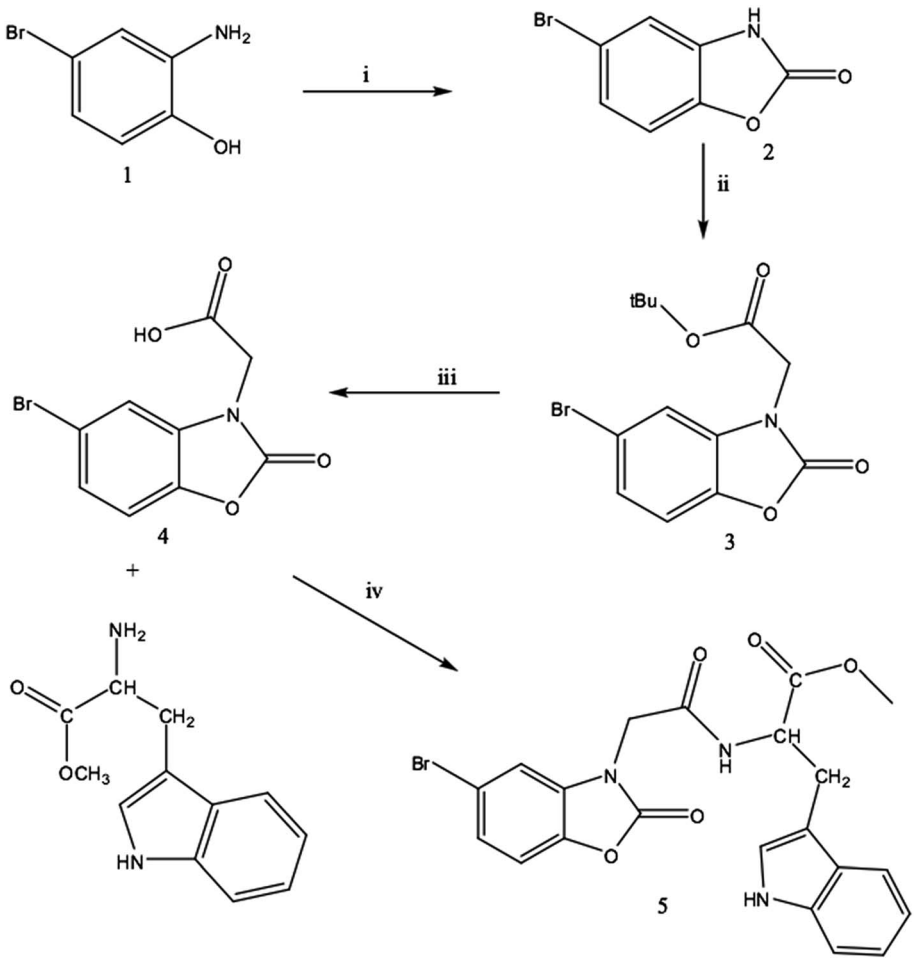

Scheme 1 Chemical synthesis. Reagents and conditions: (i) CDI, THF, rt; (ii) ^{t}butylbromoacetate, K_2CO_3, DMF, 70 °C; (iii) HCl, dioxane, AcOH, 50 °C; (iv) tryptophan methyl ester hydrochloride, EDCl, HOBt, DMF, rt.

Incubation of the freshly prepared radiocomplex in fresh human serum was done at physiological conditions *i.e.* at 37 °C (concentration 100 nM ml^{-1}) and then it was analyzed by ITLC-SG to detect any dissociation of the complex at different time intervals. Percentage dissociation of the complex was determined by calculating percentage of free pertechnetate at a particular time by using saline and acetone as mobile phases. This represents percentage dissociation of the complex at that particular time point in serum.

2.1.8. Biodistribution studies. Tissue distribution studies were performed on BALB/c mice. All the guidelines of the Institutional Animal Ethics Committee were followed during animal handling and experimentation. Radiolabelled compound was injected in mice through tail vein (10 μCi). Mice were sacrificed at six time intervals (5 min, 15 min, 30 min, 60 min, 120 min, and 1440 min), blood was collected and different organs (brain, heart, lung, liver, spleen, kidney, stomach and intestine) were dissected for analysis. Radioactivity was measured in the gamma counter. Radioactivity injected in each mouse was found out by subtracting the activity left in tail from the activity injected. Radioactivity found in each organ was expressed as percentage administered dose per gram (% ID per g) of tissue. Blood volume was calculated as 7% of the total body weight. Decay correction was applied to radioactivity measurements.

2.1.9. Preparation of mice model. The inflammatory model was prepared as per previous literature.[35–39] 10 weeks old male BALB/c mice of 22–25 g weight were taken to develop inflammation model. 40 μl of *E. coli* lipopolysaccharide (5 mg kg^{-1}) in PBS was administered intranasally in each mouse. Mice were housed under a 12 h dark–light cycle and were allowed free access of food pellets and water. After 24 h the mice were used for animal studies.

For *ex vivo* biodistribution blocking evaluation, three different concentration of TSPO ligand (PK11195) 2.5 mg kg^{-1}, 5 mg kg^{-1}, and 10 mg kg^{-1} were injected 10 min prior to ^{99m}Tc-MBIP injection (100 μl of 1 mg kg^{-1}). All the experiments were performed in triplicate set ($n = 3$). During this study 5 mg kg^{-1} blocking was found most appropriate that is why it was taken for *in vivo* imaging at 40 min post radioligand intravenous injection.

3. Result and discussion

MBIP, acetamidobenzoxazolone–indole based ligand designed on the basis of pharmacophore modeling and docking studies, has been synthesized as per Scheme 1 and radiolabelled with ^{99m}Tc for its evaluation as a diagnostic agent for TSPO targeting whose concentration is perturbed during inflammation in TSPO enriched organs. The stability of ^{99m}Tc complex, biodistribution and serum stability studies of the ligand were found appropriate for SPECT application.

Ligand based drug design makes use of the knowledge of other known ligands for same target. These ligands could provide information about minimum structural characteristics necessary for binding with biological target in terms of pharmacophoric model. This model/hypothesis could be useful in designing new ligands. Pharmacophore model was developed with TSPO ligands having benzoxazolone to understand the key features responsible for affinity. K_i values taken for all the ligands were studied against TSPO of the kidney membrane.

As per our previous findings about acetamidobenzoxazolone pharmacophore based skeleton was found suitable for new TSPO ligand which is not affected by intersubject variability. Besides that Fukaya and others[33] have also confirmed that appropriate hydrophobic/acceptor groups attached with benzoxazolone and acetamide have potential to bind TSPO selectively in nM concentration.

Different pharmacophoric features like hydrogen bond donor (D), acceptor (A), hydrophobic group (H), and aromatic ring (R) were chosen to generate the hypothesis. The 51 TSPO ligands were divided into test set and training set with 13 and 38 ligands, respectively. Ligands of these sets were aligned with each other to find the pharmacophore and thereafter PLS analysis was performed. Hypothesis AAAR showed best result in terms of predictive ability and internal validation (Fig. 1) with $R^2 = 0.95$ and standard deviation in the range of 0.237 to 0.760. This hypothesis was further utilized for designing of new ligand.

Based on these concepts we have designed MBIP as TSPO ligand. A substituent on the benzoxazolone derivative specifically at C-5 position of phenyl ring plays an important role in TSPO binding. Substitution by halogen in place of aromatic ring system at this position provides sub-nanomolar binding affinity.[33] This is the rationale behind selecting Br for C-5 position for designing the benzoxazolone ring. This has also been mentioned in literature that compound suffered from poor solubility due to phenyl substituent at acetamida side. We have tried biocompatible amino acid analogue at this position

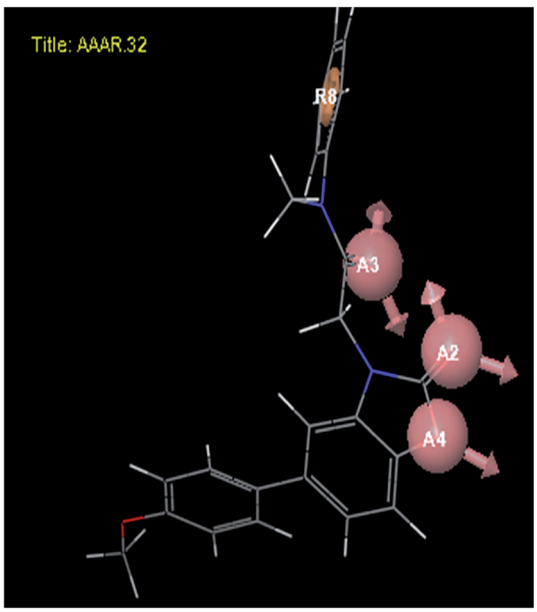

Fig. 1 Pharmacophore model AAAR used for designing TSPO ligand derived from the benzoxazolone derivatives. Pharmacophoric features with colour code: A-hydrogen bond acceptor (pink) and R-aromatic moiety (orange).

to solve solubility issue for better prospect of clinical application in future. The R contained in MBIP is also present in TSPO ligands-FGIN-127 which has nanomolar binding affinity for TSPO. Its limited *in vivo* use is due to its high lipophilicity. The designed ligand MBIP showed decreased computational log *P* (2.31) value as compared to FGIN-127 (computational log *P* = 6.94).[30]

The intersubject variability issue for MBIP has been studied computationally by taking 2 wild type PDBs (4RYO and 4RYQ) and one mutant PDB (4UC1) representing required SNP for docking studies. MBIP has shown good interactive score (G_{score}) for wild type and mutant PDBs similar to PK11195 and FEBMP which are successful ligands against intersubject variability (ESI†). The validation of docking protocol was done before docking the compounds with PDB. The ligand present in co-crystallized PDB was removed and docked with binding site. The root mean square deviation between predicted and observed X-ray crystallographic conformers was found to be around 0.5 Å predicting the reproduction of binding mode of docked compound using this docking protocol.

After designing, the next step is validation for TSPO binding/affinity which was carried out through docking studies to gain better insight of its interaction with TSPO as compared to other known TSPO ligands. MBIP demonstrated comparable or better affinity with TSPO in terms of G_{score} (−10.448 for MBIP > −7.451 to −10.15 for other known ligands) (Table 1). Both the parent ligands FEBMP and FGIN-127 have G_{score} −10.151 and −9.319, respectively on docking with TSPO. The MBIP interaction with 4RYO has been reflected in their interactions shown in 2D and 3D interaction diagram (Fig. 2). Various interactions were observed in docking including pi–pi interaction with Phe90 and Phe95, hydrogen bonding with Gly44 and Ser22. Both the aromatic rings were participating in pi–pi interactions. One hydrogen bond was observed due to NH of indole moiety in the ligand. These interactions were different from interactions of MBMP and its fluoro analog with TSPO (Try27, Tyr28, Phe19 and Try99).[19]

Table 1 Glide G_{score} of MBIP and other known TSPO ligands on docking with TSPO (PDB ID: 4RYO). Docking was performed using extra precision mode of GLIDE, Schrödinger, Maestro LLC 9.1 software

Ligand	*G*-Score
MBIP	−10.448
DAA1106	−9.493
DIAZEPAM	−7.451
DPA713	−6.180
FEBMP	−10.151
FEDAA1106	−9.809
FGIN-127	−9.319
FPBMP	−9.633
PBR28	−9.658
PBR111	−7.475
PK11195	−9.881
RO5-4864	−9.034
SSR180575	−7.992
XBD173	−9.406

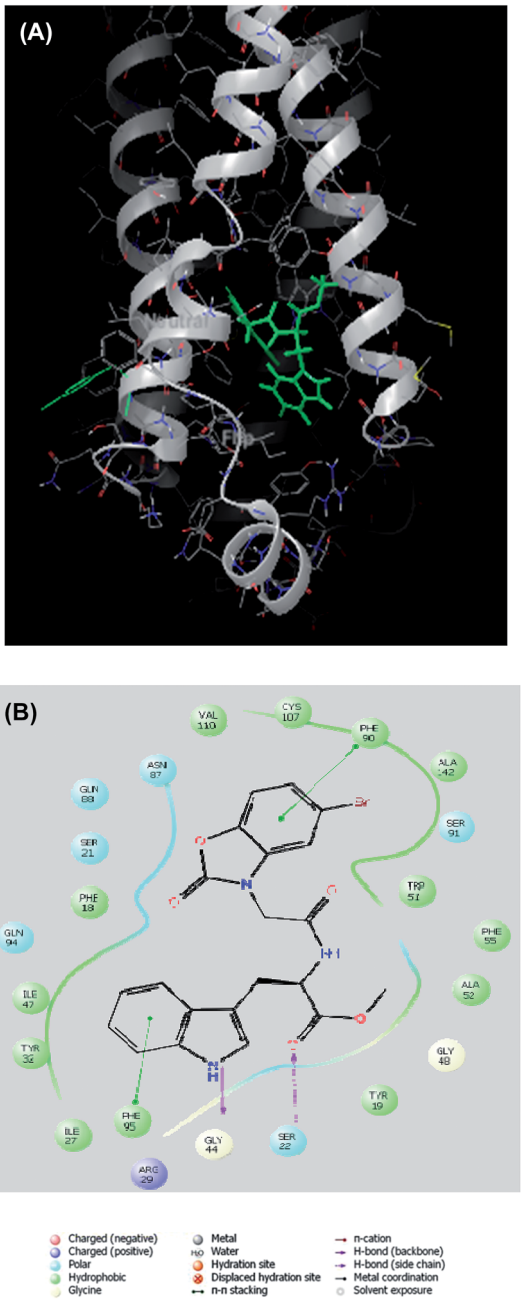

Fig. 2 3D (A) and 2D (B) interaction diagram of MBIP on docking with TSPO (PDB ID: 4RYO). Docking was performed using extra precision mode of GLIDE, Schrödinger, Maestro LLC 9.1 software. MBIP formed pi–pi interactions of aromatic rings with Phe90 and Phe95 and hydrogen bond interactions with Gly44 and Ser22.

BcTSPO-PK11195 model showed interaction between oxygen of carbonyl group of PK11195 with indole groups of Try51 and Try138, van der Waal interaction with Ser22, Tyr32, Pro42, Ile47, Phe55, Phe90, Ser91, GIn94, Cys107, Ala142 and Leu145. Few of the interaction of PK11195 as on Ser22 and Phe90 were similar to MBIP interactions with TSPO protein.[40] MBIP and FEBMP both the compounds have shown similar binding modes. The C═O of benzoxazolone forms H-bond with the Try51 in 4RYQ. This is in agreement with the interaction of PK11195 with

4RYQ. Few more interaction sites are common to MBIP in 4RYO and 4RYQ such as Ser22, Phe55, Phe90, Ser91, Gln94, Cys107, Ala142. Their glide G_{score} and their contribution from different sub interactions were found comparable (ESI†).

The precursor 2-(5-bromo-benzoxazolone)acetic acid of compound MBIP was synthesized in three steps starting from 4-bromo-2-amino phenol by the procedure reported in the literature.[33] In the last step, the ligand 2-(2-(5-bromo benzoxazolone) acetamido)-3-(1*H*-indol-3-yl)propanoate was synthesized through amidation reaction of 5-bromo-benzoxazolone acetic acid and tryptophan methyl ester hydrochloride in the presence of HOBt and EDCl. The yield of the final product was 62% and was purified using column chromatography and preparative HPLC. The retention time of final product MBIP was found to be 8.75 min. The chemical purity of the compound was determined using analytical HPLC and purity was found to be >97%. In the ^{1}H-NMR, two singlet NH peaks of same intensity were observed at 8.8 and 10.9 ppm which correspond to NH of amide and NH of indole, respectively. This indicates the successful synthesis of the proposed structure. All the eight aromatic protons of benzoxazolone and indole moieties were observed in the region 6–8 ppm. ^{13}C-NMR reflected appropriate peaks as per its formula. Three C=O peaks were observed at 172.3, 166.2 and 154.1 ppm which correspond to ester C=O, amide C=O and benzoxazolone C=O, respectively. MS run in the positive mode has peak at 496.3 $[M + Na]^{+}$ which was in accordance with the proposed structural formula. After synthesis, biological evaluation was performed by tracer method using ^{99m}Tc. The radiolabelling study was carried out with the procedure reported in our previous work.[41] Stability of the complex is one of the most important criteria for use of the ligand *in vivo* as it avoids metabolite formation and transchelation which changes the desired property for SPECT application. Complexation of the synthesized ligand with ^{99m}Tc gave sufficient stability over 24 h (Fig. 3). *In vitro* serum stability clearly indicates the stable nature of radio complex without any transchelation to serum protein like albumin which was observed to be >91% intact after 24 h (Fig. 4). Stability studies showed requisite stability of the complex to act as a SPECT agent.

Biodistribution using radiocomplex was carries out to have an idea whether the radioligand is reaching the organs of interest which are rich in TSPO and its excretion from the body. The distribution in different organs is represented as percentage of injected dose per organ at different time points. Table 2 showed the distribution of radioactive compound at six different time points post injection into the mice ($n = 3$). At 5 min, peak value of activity was recorded in all the organs. Highest % ID per g was observed in liver *i.e.* 28.87 followed by

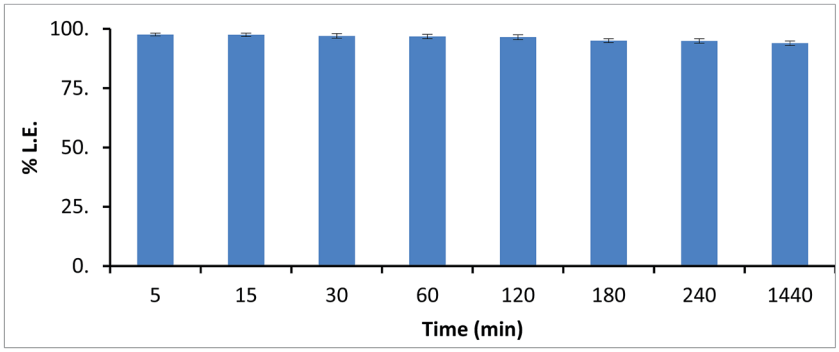

Fig. 3 Labeling efficiency (% LE) of MBIP with ^{99m}Tc. $NaTcO_4$ at pH 7 was used for labeling. 0.1 cm segment of ITLC were used after developing it in solvents acetone and PAW (pyridine, acetic acid and water in 3 : 5 : 1.5 ratio) for count measurement.

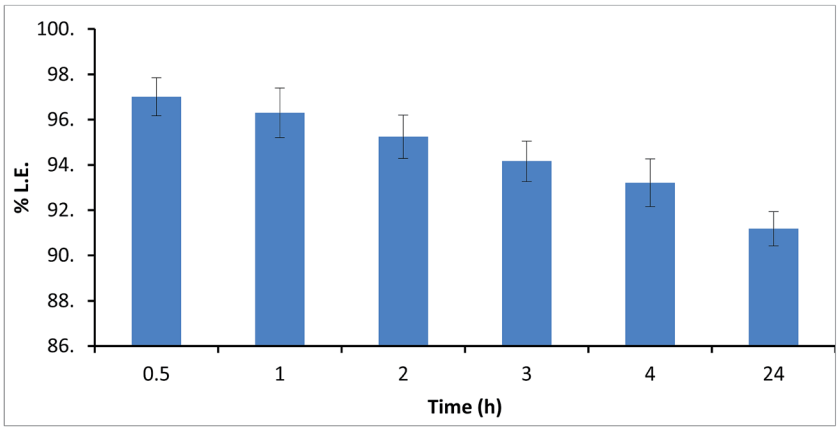

Fig. 4 Serum stability study in terms of labeling efficiency (% LE) of ^{99m}Tc-MBIP over 24 h. Studies were performed in fresh human serum from healthy volunteers at physiological conditions *i.e.* 37 °C.

Table 2 Biodistribution of ^{99m}Tc-MBIP in normal BALB/c mice. Mice ($n = 3$) received 10 μCi of ^{99m}Tc-MBIP by tail vein injection. Radioactivity uptake in different organs were measured by gamma counting and expressed as % ID per g, mean ± standard deviation

Organ/tissue	5 min	15 min	30 min	60 min	120 min	1440 min
Blood	2.23 ± 0.11	1.62 ± 0.08	1.84 ± 0.09	1.02 ± 0.09	0.98 ± 0.05	0.65 ± 0.05
Brain	0.06 ± 0.01	0.04 ± 0.01	0.04 ± 0.01	0.03 ± 0.02	0.03 ± 0.01	0.01 ± 0.01
Heart	0.72 ± 0.04	0.72 ± 0.04	0.49 ± 0.02	0.37 ± 0.02	0.02 ± 0.02	0.16 ± 0.01
Lungs	5.20 ± 0.26	4.70 ± 0.23	3.15 ± 0.16	1.33 ± 0.16	0.94 ± 0.07	0.29 ± 0.05
Liver	28.87 ± 1.44	23.12 ± 1.16	21.50 ± 1.07	18.21 ± 1.07	12.07 ± 0.91	9.62 ± 0.60
Spleen	10.25 ± 0.51	6.88 ± 0.34	5.18 ± 0.26	4.97 ± 0.26	3.42 ± 0.25	1.72 ± 0.17
Kidney	11.19 ± 0.56	4.57 ± 0.23	3.50 ± 0.17	2.27 ± 0.17	1.09 ± 0.11	0.90 ± 0.05
Stomach	0.55 ± 0.03	0.29 ± 0.01	0.46 ± 0.02	0.30 ± 0.02	0.04 ± 0.02	0.23 ± 0.01
Intestine	0.53 ± 0.03	0.45 ± 0.02	0.45 ± 0.02	0.30 ± 0.02	0.02 ± 0.02	0.08 ± 0.01

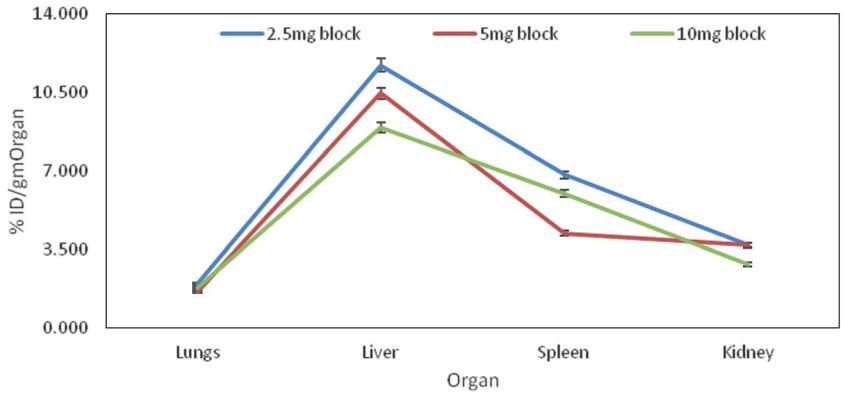

Fig. 5 ^{99m}Tc-MBIP *ex vivo* biodistribution in lung, liver, spleen and kidney at 40 min post i.v. injection with 10 min preadministration of 2.5/5/10 mg kg^{-1} PK11195 as blocking agent.

kidney, spleen and lung which were 11.19, 10.25, and 5.20, respectively. 15 min onwards spleen contained highest radioactivity after liver *i.e.* 6.88, 5.18, 4.97, 3.42, and 1.72% ID per g at 5 min, 15 min, 30 min, 60 min, 120 min, and 1440 min, respectively. Lung and kidney also have significant amount of radioligand present till 30 min *i.e.* 3.15 and 3.50% ID per g, respectively. Thereafter, radioactivity decreased sharply in lungs with 25% to 5.5% of uptake at 5 min from 60 min to 1440 min. Similar trend was observed in kidney *i.e.* 20% of the uptake at 5 min in 60 min and subsequent reduction to 8% in 1440 min. The biodistribution pattern revealed that the radioactivity is mainly localized in TSPO-expressing organs such as lung, liver, spleen, and kidney. The good uptake of radioactivity in requisite organs proves it as TPSO targeting ligand. In literature, highest uptake in liver, after intestine, has been reported for ^{99m}Tc labelled 2-quinoline carboxamide analogs.[25] ^{99m}Tc-MBIP demonstrated negligible uptake in intestine which is desirable for TSPO ligand.

In brain, small uptake of 0.06% ID per g at 5 min was observed which decreased to 0.01% at the last time point of observation. The small % ID in brain could be attributed to moderate expression of TSPO in the healthy brain. Maximum quantity of radioactivity in liver showed that the clearance of the radioligand is through hepatobiliary route.

The saturation aspect of TSPO binding site by ^{99m}Tc-MBIP has been studied by blocking with PK11195 on lung inflamed mice model. ^{99m}Tc-MBIP showed uptake in all the TSPO enriched organs. Blocking percentage in lungs and other peripheral organs was found in the range of 23–60% as per ROI derived data (ESI†) which is similar to the findings of previous ligands used in nuclear medicine. Literature reported ^{99m}Tc-labelled 2-quinoline carboxamide ligands showed only significant effect in uptake of lung but not in remaining tissues on pre-administration of PK11195.[25] PET TSPO ligands [^{18}F]-DPA-714 [17] and [^{18}F]VC701 [42] showed blocking in the range of 46–72% and 36–88%, respectively.

TSPO enriched peripheral organs have shown blocking but it was not concentration dependent for all (Fig. 5), which could be attributed to small sample size or staging of inflamed condition. Further studies with different animal models may clarify the saturation trend once blocked with cold reference like PK11195.

In summary, *in silico* studies on modified MBMP skeleton followed by facile synthesis and biological evaluation were carried out for TSPO target for SPECT application.

4. Conclusion

This work resulted in the synthesis of a new TSPO ligand 2-(2-(5-bromo benzoxazolone)acetamido)-3-(1*H*-indol-3-yl)propanoate (MBIP) for diagnostic application using SPECT. The ligand binding interaction with TSPO was calculated through MM

analysis and subsequently synthesized in four steps. MBIP formed a stable complexation with ^{99m}Tc which remained >91% stable at 24 h in serum alongwith favorable *ex vivo* biodistribution in TSPO expressing organs. Stable nature of complex, high uptake at early time points in desired organs with fast kinetics proved MBIP as potential candidate for SPECT. Further studies are required to prove its efficiency as TSPO ligands for human clinical application.

Acknowledgements

We extend special thanks to Dr A. K. Mishra, Head, Division of Cyclotron and Radiopharmaceutical Science, INMAS, Delhi, for providing us the facility to carry out experiments. We thank Dr Anshoo Gautam, Scientist D, INMAS for her support to develop animal model. This work was supported by INMAS, Delhi under Task Project ST/15-16/INM-03. There is no conflict of interest among authors of this manuscript.

References

1 R. Rupprecht, V. Papadopoulos, G. Rammes, T. C. Baghai, J. Fan, N. Akula, G. Groyer, D. Adams and M. Schumacher, *Nat. Rev. Drug Discovery*, 2010, **9**(12), 971–988.
2 R. Jean, E. Bribe, L. Knabe, A. F. Petit, I. Vachier and A. Bourdin, *Rev. Mal. Respir.*, 2015, **32**(3), 320.
3 H. A. Jones, P. S. Marino, B. H. Shakur and N. W. Morrell, *Eur. Respir. J.*, 2003, **21**, 567–573.
4 L. Veenman and M. Gavish, *Pharmacol. Ther.*, 2006, **110**(3), 503–524.
5 A. Hatori, J. Yui, L. Xie, T. Yamasaki, K. Kumata, M. Fujinaga, H. Wakizaka, M. Ogawa, N. Nengaki, K. Kawamura and M. R. Zhang, *PLoS One*, 2014, **9**(1), e86625.
6 V. Papadopoulos and L. Lecanu, *Exp. Neurol.*, 2009, **219**, 53–57.
7 V. M. Milenkovic, R. Rupprecht and C. H. Wetzel, *Mini-Rev. Med. Chem.*, 2015, **15**, 366–372.
8 L. Veenman, A. Vainshtein and M. Gavish, *Cell Death Dis.*, 2015, **6**, e1911.
9 V. Papadopoulos, M. Baraldi, T. R. Guilarte, T. B. Knudsen, J. J. Lacapère, P. Lindemann, M. D. Norenberg, D. Nutt, A. Weizman and M. R. Zhang, *Trends Pharmacol. Sci.*, 2006, **27**, 402–409.
10 J. Fan, P. Lindemann, M. G. Feuilloley and V. Papadopoulos, *Curr. Mol. Med.*, 2012, **12**, 369–386.
11 R. Lin, A. Angelin, F. da Settimo, C. Martini, S. Taliani, S. Zhu and D. C. Wallace, *Aging Cell*, 2014, **13**, 507–518.
12 J. H. Cho, J. H. Park, C. G. Chung, H. J. Shim, K. H. Jeon, S. W. Yu and S. B. Lee, *Biochem. Biophys. Res. Commun.*, 2015, **463**, 1–6.
13 E. Levin, A. Premkumar, L. Veenman, W. Kugler, S. Leschiner, I. Spanier, G. Weisinger, M. Lakomek, A. Weizman and S. H. Snyder, *Biochemistry*, 2005, **44**, 9924–9935.
14 G. Weisinger, E. Kelly-Hershkovitz, L. Veenman, I. Spanier, S. Leschiner and M. Gavish, *Biochemistry*, 2004, **43**, 12315–12321.
15 W. C. Kreisl, M. Fujita, Y. Fujimura, N. Kimura, K. J. Jenko, P. Kannan, J. Hong, C. L. Morse, S. S. Zoghbi, R. L. Gladding, S. Jacobson, U. Oh, V. W. Pike and R. B. Innis, *NeuroImage*, 2010, **49**, 2924–2932.
16 T. Yamasaki, K. Kumata, K. Yamamoto, A. Hatori, M. Takei, Y. Nakamura, S. Koike, K. Ando, K. Suzuki and M. R. Zhang, *Nucl. Med. Biol.*, 2009, **36**, 801–809.
17 C. Vicidomini, M. Panico, A. Greco, S. Gargiulo, A. R. D. Coda, A. Zannetti, M. Graman zini, G. N. Roviello, M. Quarantelli, B. Alfano, B. Tavitian, F. Dolle, M. Salvatore, A. Bru netti and S. Pappata, *Nucl. Med. Biol.*, 2015, **42**, 309–316.
18 A. K. Tiwari, J. Yui, M. Fujinaga, K. Kumata, Y. Shimoda, T. Yamasaki, L. Xie, A. Hatori, J. Maeda, N. Nengaki and M. R. Zhang, *J. Neurochem.*, 2014, **129**(4), 712–720.
19 A. K. Tiwari, M. Fujinaga, J. Yui, T. Yamasaki, L. Xie, K. Kumata, A. K. Mishra, Y. Shimoda, A. Hatori, B. Ji, M. Ogawa, K. Kawamura, F. Wang and M. R. Zhang, *Org. Biomol. Chem.*, 2014, **12**(47), 9621–9630.
20 A. K. Tiwari, B. Ji, M. Fujinaga, T. Yamasaki, L. Xie, R. Luo, Y. Shimoda, K. Kumata, Y. Zhang, A. Hatori, J. Maeda, M. Higuchi, F. Wang and M. R. Zhang, *Theranostics*, 2015, **5**(9), 961–969.
21 A. K. Tiwari, J. Yui, Y. Zhang, M. Fujinaga, T. Yamasaki, L. Xie, Y. Shimoda, K. Kumata, A. Hatori and M. R. Zhang, *RSC Adv.*, 2015, **5**(123), 101447–101454.
22 S. Tsartsalis, N. Dumas, B. B. Tournier, T. Pham, M. Moulin-Sallanon, M. C. Gregoire, Y. Charnay and P. Millet, *EJNMMI Res.*, 2015, **5**(9), 1–6.
23 F. Mattner, M. Quinlivan, I. Greguric, T. Pham, X. Liu, T. Jackson, P. Berghofer, C. J. R. Fookes, B. Dikic, M. C. Gregoire, F. Dolle and A. Katsifi, *Dis. Markers*, 2015, 729698.
24 S. Piccinonna, N. D. Enora, N. Margiotta, V. Laquintana, G. Trapani and G. Natile, *Z. Anorg. Allg. Chem.*, 2013, **639**(8–9), 1606–1612.
25 A. Cappelli, A. Mancini, F. Sudati, S. Valenti, M. Anzini, S. Belloli, R. M. Moresco, M. Matarrese, M. Vaghi, A. Fabro, F. Fazio and S. Vomero, *Bioconjugate Chem.*, 2008, **19**(6), 1143–1153.
26 S. Piccinonna, N. Marietta, N. Denora, R. M. Lacobazzi, C. Pacifico, G. Trapani and G. Natle, *Dalton Trans.*, 2013, **42**, 10112–10115.
27 N. Denora, N. Margiotta, V. Laquintana, A. Lopedota, A. Cutrignelli, M. Losacco, M. Fran co and G. Natile, *ACS Med. Chem. Lett.*, 2014, **5**, 685–689.
28 E. Cerutti, *Magn. Reson. Chem.*, 2013, **51**(2), 116–122.
29 H. C. Manning, T. Goebel, R. C. Thompson, R. R. Price, H. Lee and D. J. Bornhop, *Bioconjugate Chem.*, 2004, **15**, 1488–1495.
30 M. L. James, S. Selleri and M. Kassiou, *Curr. Med. Chem.*, 2006, **13**, 1991–2001.
31 F. Chauveau, H. Boutin, N. V. Camp, F. Dolle and B. Tavitian, *Eur. J. Nucl. Med. Mol. Imaging*, 2008, **35**, 2304–2319.
32 D. R. Owen, R. N. Gunn, E. A. Rabiner, I. Bennacef, M. Fujita, W. C. Kreisl, R. B. Innis, V. W. Pike, R. Reynolds and P. M. Matthews, *J. Nucl. Med.*, 2011, **52**, 24–32.

33 T. Fukaya, T. Kodo, T. Ishiyama, H. Kakuyama, H. Nishikawa, S. Baba and S. Masumoto, *Bioorg. Med. Chem.*, 2012, **22**, 5568–5582.
34 T. Fukaya, T. Kodo, T. Ishiyama, H. Nishikawa, S. Baba and S. Masumoto, *Bioorg. Med. Chem.*, 2013, **21**, 1257–1267.
35 Y. S. Kim, J. W. Hwang, J. H. Jang, S. Son, I. B. Seo, J. H. Jeong, E. H. Kim, S. H. Moon, B. T. Jeon and P. J. Park, *Molecules*, 2016, **21**, 392.
36 M. Starkhammar, S. K. Georen, L. Swedin, S. E. Dahlen, M. Adner and L. O. Cardell, *PLoS One*, 2012, **7**(2), e32110.
37 S. Knapp, S. Florquin, D. T. Golenbock and T. V. poll, *J. Immunol.*, 2006, **176**, 3189–3195.
38 J. Lefort, L. Motreff and B. B. Vargaftig, *Am. J. Respir. Cell Mol. Biol.*, 2001, **24**, 345–351.
39 http://www.biomodels.com/animal-models/pulmonary-disease/acute-lung-injurycopd/.
40 Y. Guo, R. C. Kalathur, Q. Liu, B. Kloss, R. Bruni, C. Ginter, E. Kloppmann, B. Rost and W. A. Hendrickson, *Science*, 2015, **347**(6221), 551–555.
41 A. K. Tiwari, D. Sinha, A. Datta, D. Kakkar and A. K. Mishra, *Chem. Biol. Drug Des.*, 2011, **77**, 388–392.
42 G. D. Grigoli, C. Monterisi, S. Belloli, V. Masiello, L. S. Politi, S. Valenti, M. Paolino, M. Anzini, M. Matarrese, A. Cappelli and R. M. Moresco, *Mol. Imaging*, 2015, **14**, 1–9.